Food & Function

Chitosan reduces vitamin D bioaccessibility in food emulsions by binding to mixed micelles

Journal:	*Food & Function*
Manuscript ID	FO-ART-09-2019-002164.R1
Article Type:	Paper
Date Submitted by the Author:	30-Nov-2019
Complete List of Authors:	McClements, David; University of Massachusetts, Food Science Tan, Yunbing; University of Massachusetts, Food Science Li, Ruyi; State Key Laboratory of Food Science and Technology, Liu, Chengzhen; University of Massachusetts, Food Science Muriel Mundo, Jorge; University of Massachusetts, Food Science Zhou,, Hualu ; University of Massachusetts, Food Science Liu, Jinning; University of Massachusetts, Food Science

Chitosan reduces vitamin D bioaccessibility in food emulsions by binding to mixed micelles

Yunbing Tan[1], Ruyi Li[2], Chengzhen Liu[3], Jorge Muriel Mundo[1], Hualu Zhou[1], Jinning Liu[1], and David Julian McClements[1*]

[1]*Department of Food Science, University of Massachusetts Amherst, Amherst, MA 01003, USA*

[2]*State Key Laboratory of Food Science and Technology, Nanchang University, Nanchang, Jiangxi 330047, PR China*

[3]*College of Food Science and Engineering, Ocean University of China, Qingdao, Shandong 266003, PR China*

Submitted: September, 2019

Journal: Food & Function

**Correspondence to: David Julian McClements, Biopolymers and Colloids laboratory, Department of Food Science, University of Massachusetts, Amherst, MA 01003, USA. E-mail: mcclements@foodsci.umass.edu*

Abstract

Consumption of sufficiently high quantities of dietary fibers has been linked to a range of health benefits. Recent research, however, has shown that some dietary fibers interfere with lipid digestion, which may reduce the bioavailability of oil-soluble vitamins and nutraceuticals. For this reason, we examined the impact of a cationic polysaccharide (chitosan) on the bioaccessibility of vitamin D using the standardized INFOGEST *in vitro* digestion model. The vitamin D was encapsulated within an emulsion-based delivery system that contained whey protein-coated corn oil droplets. Our results showed that chitosan promoted severe droplet flocculation in the small intestine and reduced the amount of free fatty acids detected using a pH-stat method. However, a back-titration of the digested sample showed that the lipids were fully digested at all chitosan levels used (0.1-0.5%), suggesting that chitosan may have bound some of the free fatty acids released during lipid digestion. The presence of the chitosan decreased the bioaccessibility of vitamin D by about 37%, but this effect did not depend strongly on chitosan concentration (0.1-0.5%). It was hypothesized that chitosan bound to the vitamin-loaded mixed micelles and promoted their precipitation. The knowledge gained in this study might provide useful insights in designing emulsion-based delivery systems with high vitamin bioaccessibility.

Keywords: chitosan; emulsion; nanoemulsion; vitamin D; bioaccessibility; *in vitro* digestion

1. Introduction

There has been considerable interest in the food industry in the design of functional foods and beverages that not only taste good, but also have specific health benefits [1]. A number of approaches are being utilized to create these healthier versions of processed foods. One approach is to decrease the levels, or at least reduce the negative effects, of food ingredients that have been linked to increased health risks, such as fat, sugar, and salt [1]. Another approach is to control the structural organization of the constituents within foods so as to alter their behavior inside the gastrointestinal tract (GIT). An example of this approach is to create foods in which the macronutrients are digested more slowly, thereby inhibiting glucose or lipid spikes in the blood that may lead to diabetes or heart disease [2, 3]. Yet another approach is to fortify foods with bioactive ingredients that have been linked to beneficial health effects, such as vitamins, minerals, and nutraceuticals [4, 5]. For example, vitamin D is vital for bone health and other critical physiological functions [6], but in many countries, some segments of the population are deficient in this essential micronutrient [7]. Nevertheless, the amount of fortification must be carefully controlled because excessive vitamin D intake can have adverse health outcomes, such as gastrointestinal disorders and kidney dysfunction [8, 9]. For this reason, the design of food matrices that can regulate the release and absorption of micronutrients like vitamin D is of great interest to the modern food industry [10].

The purpose of the current study was to examine the impact of a dietary fiber (chitosan) on the bioavailability of vitamin D encapsulated within emulsion-based delivery systems. In general, dietary fibers are claimed to have a number of potentially beneficial health effects [11-16]. For instance, they can inhibit glucose absorption, promote satiety, and thereby reduce overall calorie consumption [17]. Dietary fibers have also been shown to modulate the gut microflora [18],

which is claimed to promote a healthy immune system and reduce the susceptibility to certain chronic diseases [19]. Dietary fibers have also been shown to modulate the rate and extent of lipid digestion in emulsion-based delivery systems [20, 21], which may impact the bioavailability of encapsulated oil-soluble vitamins. Several possible mechanisms have been proposed to account for the ability of dietary fibers to interfere with lipid digestion: (1) formation of coatings around oil droplets [22, 23];(2) promotion of droplet flocculation [24]; (3) thickening or gelling of gastrointestinal fluids [25-27]; (4) binding to critical components in the lipid digestion process, such as bile salts, free fatty acids [24, 28], digestive enzymes [29], and, calcium ions [30]; (5) binding to mixed micelles [31].

The tendency for specific dietary fibers to be involved in these different mechanisms depends on their molecular and physicochemical characteristics (such as molecular weight, charge, conformation, and solubility), as well as food matrix properties (such as composition and structure). We hypothesized that chitosan could impact the bioaccessibility of vitamin D by interfering with the lipid digestion process by one or more of the above mechanisms.

Food-grade chitosan is commonly produced by deacetylation of the chitin found in the shells of crustaceans, such as crabs and shrimps [32, 33]. It is one of the few positively charged polysaccharides available and so has been widely used as a functional ingredient in foods and other commercial products for its binding, structure building, film forming, and other functional attributes [34]. Chitosan is widely used in research studies but does not currently have GRAS approval for use as a food additive in the US [35], although it is used in some other countries [36] The positive charge on chitosan molecules is due to aliphatic amino groups that are protonated ($-NH_3^+$) under acidic conditions: $pK_a \sim 6\text{-}7$ [37]. The cationic nature of chitosan is believed to be responsible for many of its physiological effects in the human gut after digestion. Several studies

have shown that chitosan can inhibit lipid digestion and reduce the bioaccessibility of hydrophobic bioactives (such as curcumin) [38, 39]. These effects have been attributed to some of the physicochemical mechanisms listed earlier. For instance, cationic chitosan can form a protective coating around anionic oil droplets, or promote their flocculation, which inhibits lipid digestion by reducing the ability of lipase to reach the lipid phase [40]. Besides, chitosan can bind to anionic free fatty acids and bile salts [31], which might alter the number of nutraceutical-loaded mixed micelles available for adsorption in the upper gastrointestinal tract (GIT).

The main objective of the current study was therefore to examine the impact of chitosan on the gastrointestinal fate of vitamin D-loaded oil droplets in emulsion-based delivery systems. In particular, we used the standardized INFOGEST simulated GIT model to examine the impact of chitosan on lipid digestion and vitamin bioaccessibility [41]. The results obtained from this study may facilitate the design of more effective emulsion-based delivery systems for oil-soluble vitamins and other non-polar bioactive agents.

2. Materials and Methods

2.1. Materials

Corn oil (Mazola, ACH Food Companies, Memphis, TN, USA) was obtained from a supermarket. Whey protein isolate (WPI) was provided by Agropur Inc (Eden Prairie, MN). Chitosan (Chitoclear cg 800, degree of deacetylation >75%, viscosity 600-1200 mPa·s) was provided by Primex ehf. (Siglufjordur, Iceland). Vitamin D_3 (1,0 Mill. I.U./g) was supplied by BASF (Ludwigshafen, Germany). Porcine gastric mucin, pepsin from porcine gastric mucosa (250 units/mg), pancreatin from porcine pancreas, porcine lipase (100-400 units/mg), porcine bile extract, and bile acid assay kit were purchased from the Sigma-Aldrich Company (St. Louis, MO, USA). Ethyl alcohol (ACS/USP grade) was purchased from Pharmco Products, Inc.

(Shelbyville, KY, USA). All other chemicals and reagents (analytical grade or higher) were purchased from either Sigma-Aldrich or Fisher Scientific (Pittsburgh, PA, USA). Double distilled water was produced by a laboratory water-purification system (Nanopure Infinity, Barnstaeas International, Dubuque, IA, USA) and was used to prepare all solutions in this study.

2.2. Emulsion Preparation

Oil-in-water emulsions were prepared according to a method reported previously [42]. An aqueous phase was prepared by dispersing powdered WPI into buffer solution (5 mM phosphate, pH 7.0) and then stirring for at least 3 hours at ambient temperature. The resulting solution was then stored at 4 °C overnight to completely hydrate the protein. The aqueous phase was filtered through Whatman qualitative filter paper (Fisher Scientific) before being used to remove any insoluble matter. The mixture of oil and aqueous phases was first subject to 2-min blending by a high-speed mixer (M133/1281-0, Biospec Products, Inc., ESGC, Switzerland) at 10,000 rpm, and then homogenized by passing through a microfluidizer (M110Y, Microfluidics, Newton, MA) at an operation pressure of 12,000 psi for five times. The final composition of the emulsion was 10 wt% oil phase (2 wt% vitamin D in corn oil) and 90 wt% aqueous phase (1.11 wt% WPI in buffer solution). This led to a WPI concentration of 1 wt% in the final emulsion.

2.3. Chitosan Solution Preparation

A chitosan stock solution was prepared by dissolving 1 wt% chitosan in 0.5% (v/v) acetic acid solution and then storing at 4 °C overnight to ensure complete hydration. Any insoluble matter was then removed from this solution by centrifugation (Sorvall Lynx 4000 centrifuge, Thermo Scientific, Waltham, MA, USA) at 15,000 rpm for 30 min at room temperature.

130 **2.4 Emulsion and Chitosan Mixing Method**

131 The chitosan stock solution was diluted with different amounts of 0.5% (v/v) acetic acid
132 solution to obtain a series of solutions containing different chitosan levels (0%, 0.2%, 0.4%, 0.6%,
133 0.8% and 1%). These solutions were then mixed with the emulsions at a 1:1 (v/v) ratio by adding
134 the emulsions dropwise into beakers containing the chitosan solutions. The resulting mixtures were
135 then stirred for 5 min to ensure they were homogenous and then placed at room temperature
136 overnight before *in vitro* digestion.

137 **2.5. Particle Size Measurements**

138 The particle size distribution of the emulsions was determined using laser diffraction
139 (Mastersizer 2000, Malvern Instruments Ltd., Malvern, Worcestershire, UK). Samples were
140 diluted in aqueous solutions and stirred in the dispersion unit at a speed of 1200 rpm to ensure
141 homogeneity. A 1:1 (v/v) mixture of 0.5% (v/v) acetic acid and phosphate buffer (5 mM, pH 7.0)
142 was used to dilute the initial samples. Double distilled water with pH adjustment was used for the
143 mouth (pH 4.8) and stomach (pH 3) samples. Phosphate buffer (5 mM, pH 7.0) was used to dilute
144 the small intestine samples. The refractive index of the corn oil used in the calculations was 1.472.
145 Average particle sizes are reported as the surface-weighted mean diameter ($D_{3,2}$). The particle size
146 of the mixed micelle samples was measured by dynamic light scattering (Zetasizer, Nano ZS series,
147 Malvern Instruments Ltd.). Phosphate buffer (5 mM, pH 7.0) was used to dilute the samples prior
148 to analysis to avoid multiple scattering effects.

149 **2.6. Particle Surface Potential Measurements**

150 The surface potential (ζ-potential) of the particles in the emulsions was measured using
151 electrophoresis (Zetasizer Nano ZS series, Malvern Instruments Ltd.). Prior to analysis, the
152 emulsions were diluted with the same solutions used for the laser diffraction measurements.

153 **2.7. Confocal Microscopy**

154 Confocal microscopy images were acquired according to a method described previously [43].
155 Prior to measurement, the oil phase was dyed with Nile red solution (1 mg Nile red in 1 ml
156 ethanol) at a ratio of 1:20 (v/v) of dye to oil phase. An aliquot (5 μL) of sample was put onto a
157 microscope slide and then a coverslip was placed on top. The excitation and emission
158 wavelengths used for Nile red fluorescence analysis were 543 and 605 nm, respectively. The
159 microscopy images were acquired using a confocal scanning laser microscope (Nikon D-Eclipse
160 C1 80i, Nikon, Melville, NY, USA) with a 60× oil immersion objective lens. The images
161 obtained were stored and analyzed using the instrument software (NIS-Elements, Nikon,
162 Melville, NY).

163 ***2.8. In vitro* Digestion**

164 The chitosan-emulsion mixtures were passed through a simulated GIT model based on the
165 standardized INFOGEST method [41]. All solutions were preheated to 37 °C prior to use and the
166 whole GIT procedure was performed at this temperature.

167 *Mouth Phase*: Preheated simulated saliva fluid containing 0.003 g/ml mucin was mixed 1:1
168 (v/v) with the test samples. The sample was then agitated using a thermally-incubated shaker
169 (Model 4080, New Brunswick Scientific, New Brunswick, NJ, USA) for 2 min at a shaking
170 speed of 100 rpm.

171 *Stomach Phase*: The sample from the mouth phase was mixed 1:1 (v/v) with simulated
172 gastric fluids containing pepsin (2000 U/ml in the final digestion mixture). After adjusting to pH
173 3.0, the sample was then agitated using the same incubated shaker for 2 h at 100 rpm.

174 *Small Intestine Phase*: The sample from the stomach phase was mixed 1:1 (v/v) with
175 simulated intestinal fluids containing bile salts (10 mM in the final mixture) and pancreatic

enzymes (trypsin activity of 100 U/ml and lipase activity of 2000 U/ml in the final mixture). After adjusting to pH 7.0, the sample was incubated in a water bath for 2 h with continuous stirring. During this time, an automatic titration unit (Metrohm, USA, Inc.) was used to maintain the sample at pH 7.0 by adding alkaline solution (0.25 M NaOH) to titrate the free fatty acids (FFAs) released. The volume of alkaline solution required to achieve neutralization was recorded and used to calculate the % of FFAs generated. A back titration to pH 9.0 was also carried out to determine the total level of free fatty acids released (since some of them may be protonated at neutral pH). A blank test was carried out using the same composition as the sample being tested but without the oil to determine the contribution of any non-lipid components to the titration curves. After 2 h of digestion under small intestine conditions, an aliquot of intestine sample was centrifuged (Sorvall Lynx 4000 centrifuge, Thermo Scientific, Waltham, MA, USA) at 30,970 ×g (18,000 rpm) for 50 min at 4 °C to separate the micelle phase.

2.9. Direct Mixing of Micelle and Chitosan

In one series of experiments, we aimed to determine the impact of adding chitosan to the mixed micelles formed during digestion. To achieve this, a corn oil-in-water emulsion (5% oil) was subjected to the above *in vitro* digestion procedure, and then the resulting mixed micelle phase was collected after centrifugation. Different amounts of chitosan stock solution (1 wt.%) was then mixed with the mixed micelle samples to reach 0%, 0.0125%, 0.025%, 0.03%, 0.0375%, 0.05% and 0.0625% of chitosan, which is similar to the chitosan levels present in the chitosan-emulsion mixtures after *in vitro* digestion. The mixed micelle-chitosan mixtures were then placed in the incubated shaker at 37 °C at 100 rpm for 2 h. Afterwards, the micelle-chitosan mixtures were centrifuged (Sorvall Lynx 4000 centrifuge) at 30,970 ×g (18,000 rpm) for 30 min at 4 °C to precipitate the sediment. The vitamin D concentration in the micelle-chitosan mixtures

and the supernatants formed after centrifugation were measured using the method described in the following section. The mass of the sediment was weighed after oven-drying at 37 °C overnight. The percentage of sediment formed was then calculated using the following expression:

$$\text{Sediment percentage} = 100 \times \frac{m_{sediment}}{m_{mixture}}$$

Here, $m_{mixture}$ and $m_{sediment}$ are the mass of the micelle-chitosan mixture and the sediment, respectively.

2.10 Vitamin D Measurement

The extraction and analysis of the vitamin D concentration was carried out using a protocol based on a previous study [44]. The vitamin D was extracted using an organic solvent consisting of a 1:1 (v/v) mixture of hexane and ethanol for three times. After being treated using a saturated sodium chloride solution, the combined extracts were dried under a nitrogen atmosphere and then re-dissolved in HPLC-grade methanol. After being passed through a 0.45 μm filter to remove any particles (VWR International, Philadelphia, PA, USA), the samples were analyzed by HPLC.

A reverse phase-HPLC system (Agilent 1100 series, Agilent Technologies, Santa Clara, CA, USA) with a Zorbax SB-C18 column (4.6×250 mm, 5 μm, Agilent Technologies, Santa Clara, CA, USA) was used to carry out the separation and analysis. The mobile phase consisted of a methanol and water mixture (95:5, v/v), and a flow rate of 1 ml/min was used. After injection of 20 μL of sample, the absorbance of the eluent was monitored at 265 nm.

The vitamin bioaccessibility (%) was calculated from measurements of the vitamin D concentrations in the total digest and in the mixed micelles:

$$\text{Bioaccessiblity} = 100 \times \frac{C_{micelle}}{C_{digest}}$$

Here, $C_{micelle}$ and C_{digest} are the concentrations of vitamin D in the mixed micelle phase and in the total digest collected after the simulated small intestine phase, respectively.

2.11. Statistical Analysis

The digestion process and all measurements were carried out in triplicate, while the emulsion preparation was carried out in duplicate. The means and standard deviations were calculated by combining the data from these different measurements. Depending on the homogeneity of the variances, either a Duncan test (homogenous) or Dunnett's T3 test (inhomogeneous) was used in the analysis of variance (ANOVA) at a confidence level of 95% to determine the statistical differences among treatments. Statistical calculations were carried out using commercial software (SPSS, IBM Corp., Armonk, NY, USA).

3. Results and Discussion

3.1. Physical and Structural Properties During *In vitro* Gastrointestinal Digestion

Initially, corn oil-in-water emulsions containing different chitosan concentrations were prepared. These mixtures were then passed through the *in vitro* digestion model to obtain a better understanding of their potential gastrointestinal fate, especially the impact of the chitosan on lipid digestion and vitamin bioaccessibility. The particle size, surface charge, and microstructure of the emulsion-chitosan mixtures were measured in each stage of the GIT model.

Initial: The emulsion-chitosan mixtures were prepared by adding the corn oil emulsion (in phosphate buffer, pH 7) drop-by-drop into the chitosan solution (in acetic acid solution, pH 3.7). The resulting solutions had pH values ranging from 3.9 to 4.6, increasing with decreasing chitosan concentration. The surface charge of the particles in all of the emulsions was highly

243 positive. The pure emulsion (no chitosan) had a surface charge of +48.8 mV (Fig. 3), because the
244 final pH was below the isoelectric point of the adsorbed proteins (pI ≈ 5). The pure emulsion had
245 a monomodal distribution and a mean particle diameter of 148 nm, which is fairly similar to that
246 of the original emulsion *i.e.,* 139 nm (Figs. 1 and 2a). The confocal microscopy images showed
247 that these emulsions contained fine oil droplets that were evenly distributed throughout the
248 samples (Fig. 4). These results indicate that the pure emulsion was stable under these pH
249 conditions, which is probably due to the strong electrostatic repulsion between the highly
250 cationic droplets.

251 In the presence of chitosan, the positive surface potential of the emulsions remained
252 relatively high and positive (+41.7 to +47.3 mV) with increasing chitosan concentration (0.1-
253 0.5 %) (Fig. 3). This effect may have been because the chitosan did not bind strongly to the
254 droplet surfaces under these acidic conditions because both the chitosan and lipid droplets had
255 strong positive charges, leading to an electrostatic repulsion. In addition, as the pH increased
256 from 4.1 to 4.6, and therefore moved closer to the isoelectric point of the adsorbed whey
257 proteins, some of the cationic chitosan molecules could have bound to anionic patches formed on
258 the protein-coated droplet surfaces [45]. As a result, the net positive charge remained relatively
259 high. The confocal microscopy images suggest that appreciable droplet flocculation occurred in
260 the emulsions at all chitosan levels used, which is most likely a result of bridging or depletion
261 flocculation [45, 46]. The extent and nature of flocculation depended on the chitosan concentration.
262 At low chitosan levels (0.1%), severe droplet flocculation occurred (Fig. 4) and the emulsions
263 visually separated into a cream layer on top and a serum layer at the bottom (Fig. 5).
264 Surprisingly, the measured mean particle diameter only increased slightly to 156 nm in the
265 presence of 0.1% chitosan (Fig. 1), which suggests that either the flocculated droplets were only

held together by relatively weak reversible attractive interactions, or that only a small fraction of the droplets were flocculated.

When the chitosan concentration was increased to 0.3%, the flocculated oil droplets appeared to be more evenly spread (less clumping) and the emulsions showed less phase separation (Figs 4 and 5). In this case, the mean particle diameter increased significantly ($p < 0.05$) to 286 nm (Fig. 1) and the particle size distribution became bimodal. These results suggest that the oil droplets were more strongly aggregated to each other and formed a 3D-network that was more resistant to gravitational separation. At 0.4 and 0.5% chitosan, there was some evidence of clumping of the flocculated droplets, a steep increase in mean particle diameter, and a shift in the particle size distribution to higher values (Figs. 1 to 3). These effects may have been due to increasing bridging and/or depletion flocculation as the chitosan level was increased [46, 47].

Mouth: The physical and structural properties of the samples changed appreciably after exposure to the oral phase. After mixing with the simulated salivary fluids, the solutions had pH values from 4.5 to 5.1. The pure emulsion was unstable under mouth conditions with visible phase separation, an increase in mean particle diameter ($D_{3,2}$ = 9.7 μm), and evidence of floc formation in the microscopy images (Figs. 1, 4 and 5). This effect may have been because of the relatively low surface potential (ζ = -0.17 mV) of the protein-coated oil droplets near the isoelectric point of the proteins, which led to a relatively weak electrostatic repulsion between them.

The addition of chitosan improved the stability of the emulsions by an amount that depended on the concentration used (Fig. 5). As the chitosan level was increased, the mean particle diameter decreased reaching a value of 331 nm at 0.3% chitosan level (Fig. 1), but a broad particle size distribution was observed (Fig. 2d). This effect may have been due to the

289 ability of the chitosan molecules to adsorb to the surfaces of the protein-coated oil droplets,
290 increase their positive charge, and strengthen the electrostatic repulsion between them. This
291 hypothesis is supported by the observation that the ζ-potential of the droplets became
292 increasingly positive as the chitosan level increased (Fig. 3). Nevertheless, the confocal
293 microscopy images showed that the protein-coated oil droplets were still highly flocculated in
294 the presence of chitosan (Fig. 4). These results suggest that there were still some bridging and/or
295 depletion flocculation at high polysaccharide levels, but the flocs formed were weak enough to
296 dissociate when the samples were diluted for the particle size measurements.
297 *Stomach:* In the stomach phase, the emulsion samples were exposed to highly acidic
298 conditions (pH 3), as well as digestive enzymes (pepsin). All the samples were highly unstable to
299 droplet aggregation (Figs. 1, 2, and 4) and phase separation (Fig. 5). The mean particle diameter
300 was relatively high (> 7 μm) at all chitosan levels (0 to 0.5%) (Fig. 1). Droplet aggregation was
301 probably a result of changes in electrostatic interactions, bridging flocculation, and protein
302 digestion. After exposure to the stomach phase, the ζ-potential of the particles was positive in all
303 the samples, increasing from +5.3 mV in the absence of chitosan to +23.2 mV in the presence of
304 0.5%, chitosan. One might have expected that this large increase in particle charge would have
305 led to stronger electrostatic repulsion between the oil droplets, but there was not a major change
306 in particle aggregation with increasing chitosan levels. This phenomenon might be explained by
307 a number of factors: (1) the change in pH caused partial or full displacement of the chitosan from
308 the oil droplet surfaces; (2) the dilution of the samples reduced the amount of chitosan coating
309 the droplet surfaces, thereby promoting bridging; (3) the digestion of the adsorbed proteins by
310 pepsin reduced the stabilizing effects of the emulsifier; and (4) the higher ionic strength of the
311 gastric fluids screened the electrostatic repulsion [48].

312 *SI-Initial:* Since pH is known to play a critical role in determining the physical and
313 structural properties of protein-stabilized emulsions [49], we measured the properties of the
314 samples at the beginning of the small intestine phase before adding the digestive enzymes and
315 bile salts. This was accomplished by adjusting the sample collected after the stomach phase to
316 pH 7. The properties of all the samples changed appreciably when the pH was increased. The
317 average mean particle diameter of the pure emulsion decreased steeply to 281 nm (Fig. 1), and
318 populations of both small and large particles were seen in the particle size distribution (Fig. 2a).
319 This result matched with the confocal microscopy images, which showed most of the flocs were
320 dispersed into small oil droplets with only a few large droplets (Fig. 4). The breakdown of the
321 flocs can mainly be attributed to an increase in the electrostatic repulsion between the droplets
322 due to an increase in their surface potential to a high negative value (-37.5 mV) (Fig. 3). The fact
323 that there were large individual oil droplets present suggests that some coalescence occurred
324 within the mouth and/or stomach phases. Visual observation of the pure emulsions indicated that
325 they were stable at the beginning of the small intestine phase (Fig 5). Overall, these results
326 suggest that most of the oil droplets stayed intact and were evenly dispersed throughout the
327 samples.

328 In contrast, the emulsions containing chitosan became more unstable when they were
329 moved from the stomach phase to the initial part of the small intestine phase. Visual observations
330 showed that all these emulsions underwent phase separation, with a white cream layer on top and
331 a clear serum layer at the bottom (Fig. 5). The addition of chitosan significantly ($p < 0.05$)
332 increased the mean particle diameter of these samples, with the effect becoming more
333 pronounced with increasing chitosan concentration (Fig. 1). Extensive droplet flocculation was
334 also observed in the confocal microscopy images (Fig. 4). This effect can be attributed to at least

two phenomena. First, chitosan is slightly positively charged at pH 7 whereas the protein-coated droplets are strongly negatively charged, thereby promoting bridging flocculation. Second, chitosan loses most of its positive charge under neutral conditions (pK_a around 6.5), which causes it to precipitate. These two mechanisms are supported by the electrophoresis measurements, which show that the negative charge on the particles decreased with increasing chitosan concentration: from -37.5 mV in the absence of chitosan to -2.5 mV in the presence of 0.5% chitosan (Fig. 3). In summary, the presence of the chitosan appears to promote the aggregation of the oil droplets.

SI-End: The properties of the samples were measured again after bile salts and digestive enzymes were added and the samples were then incubated for 2 hours. At the end of the small intestinal phase, the mean particle diameter of the pure emulsions increased significantly ($p < 0.05$) to around 970 nm (Fig. 1). This change might be brought about by the digestion of the lipid droplets and the formation of large colloidal structures like vesicles and insoluble calcium soaps [50]. The magnitude of the surface potential in the pure emulsion sample increased slightly to -44.0 mV (Fig. 3), which has been attributed to the presence of colloidal particles comprised of anionic constituents, such as free fatty acids, bile salts, and peptides [50]. The confocal microscopy images indicated that most of the oil droplets had been digested by the end of the small intestine phase (Fig. 4).

Compared to the beginning of the small intestinal phase, the mean particle diameters of the samples containing chitosan decreased greatly after the small intestine phase. Even so, the $D_{3,2}$ value still increased with increasing chitosan concentration: from 0.97 μm in the absence of chitosan to 3.33 μm in the presence of 0.5% chitosan (Fig. 1). The confocal microscopy images also indicated that most of the oil droplets were digested at all chitosan concentrations, but that

there were slightly more lipid-rich particles remaining at higher chitosan levels (Fig. 4). Interestingly, these results show that even though the emulsions containing chitosan were highly flocculated at the beginning of the small intestine phase, most of the oil droplets were still digested by the end. Unlike at the beginning of the small intestine phase, the surface potential of the samples containing chitosan was highly negative and did not change much at different chitosan levels ranging from -32.0 to -40.6 mV. This effect can be attributed to the relatively high level of anionic components in the small intestine phase, such as free fatty acids and bile salts. Presumably, these components bound to the positively charged chitosan molecules and neutralized their charge.

The surface potential of the mixed micelles collected after centrifugation of the digest were also measured (Fig. 4). The ζ-potential of the mixed micelle samples were fairly similar to those of the equivalent whole intestinal samples, suggesting that the mixed micelles dominated the overall charge characteristics.

3.2. Release of Free Fatty Acids During Intestinal Digestion

The release of free fatty acids (FFA) from the emulsions within the small intestine phase was recorded using a pH stat method by adding increasing volumes of alkaline solution to maintain a neutral pH. The FFA-time release profiles are shown in Fig. 6a and the final FFA values are shown in Fig. 6b. The measured FFA values increased rapidly during the first few minutes of digestion but then increased more steadily at longer times. In general, the level of FFAs detected in the pure emulsions was higher than that detected in the emulsions containing chitosan. For instance, the final FFA value was around 65% for the pure emulsion, whereas it was around 47% to 53% for the emulsions containing chitosan. These results appear to be inconsistent with the confocal microscopy images, which showed that most of the oil droplets

had been fully digested by the end of the small intestine phase (Fig. 4). This apparent inconsistency might be due to the fact that a fraction of the FFAs were not ionized at pH 7 and so could not be titrated. To test this hypothesis, a back titration to pH 9 was carried out, since this protocol has previously been shown to be capable of measuring all of the FFAs present [51]. After back titration, the final FFA values of all the samples (102% to 115%) suggested that full lipid digestion had occurred. This result suggests that chitosan did not inhibit lipid digestion, but instead altered the amount of FFAs that could be detected by the pH stat method at pH 7. Presumably, the cationic chitosan molecules bind to any anionic free fatty acids at neutral pH thereby reducing the number of titratable protons (H^+) released.

In previous studies, it has been suggested that chitosan can inhibit lipid digestion through a number of mechanisms, including inducing oil droplet flocculation, forming coatings around oil droplets, or binding to digestive components (like enzymes or bile salts) [52]. Our current results suggest that some of these earlier observations might have been because a back-titration step was not carried out. As a result, not all of the FFAs released during lipid digestion were measured. In addition, most of the earlier studies were carried out using an *in vitro* digestion method that contained different levels of digestive enzymes, calcium, and other components to the standardized INFOGEST digestion method used in the current study [41]. In particular, the INFOGEST method uses higher levels of pancreatic enzymes and lower levels of calcium, which may alter the rate and extent of lipid digestion. Having said this, our results still show that chitosan does interfere with the lipid digestion process under neutral conditions.

3.4. Vitamin Bioaccessibility

The vitamin D bioaccessibility in the emulsion-chitosan mixtures was measured after they had been passed through the entire *in vitro* simulated digestion model (Fig. 7). The pure

emulsion had the highest bioaccessibility (68.5%), which is quite similar to the value published previously (75.2%) for a fairly similar system [44]. The addition of chitosan significantly ($p < 0.05$) reduced the bioaccessibility of the vitamin in the emulsion (37.5% to 47.0%), but the decrease did not depend strongly on chitosan concentration. There have been few previous studies on the impact of chitosan on the bioaccessibility of lipophilic bioactives. One study showed that chitosan enhanced the bioaccessibility of curcumin [24], while others showed that it reduced the bioaccessibility of EGCG and carotenoids [52, 53]. These differences might be due to differences in the bioactive agents, food matrices, and *in vitro* digestion models used by different researchers.

In general, the bioaccessibility of oil-soluble vitamins in emulsion-based delivery systems is governed by two processes: (1) their release from the oil droplets due to digestion of the triglycerides; (2) their solubilization within the mixed micelles. Several previous studies have suggested that there is a relationship between the extent of lipid digestion and the bioaccessibility of hydrophobic bioactives [24, 38, 52]. As shown by Figs. 4 and 6, however, the majority of the oil phase was fully digested by the enzymes in this study, so all of the vitamin D should have been released from the oil droplets. Thus, the decrease in vitamin bioaccessibility observed in the presence of chitosan was probably not due to its impact on lipid digestion. Instead, we hypothesized that it was related to the micellization process. This process may be altered through a number of physicochemical mechanisms: (1) modification of the properties of the mixed micelles formed, such as the size of their hydrophobic domains [42]; (2) reduction of the total amount of mixed micelles formed during digestion [54]; and, (3) precipitation of some of the mixed micelles [55]. In this study, we believe that the cationic chitosan molecules bound to the anionic vitamin-loaded mixed micelles, which led to the formation of large insoluble aggregates. These aggregates would be removed from the digest during the centrifugation process and so would not

be detected as part of the mixed micelle phase. This hypothesis is supported by visual observations of the samples, which showed that an increasing amount of sediment was formed at the bottom of the tubes as the chitosan concentration was increased (Fig. 5). It should be noted, however, that these precipitated mixed micelles might be liberated when the chitosan is digested by the gut microbiota in the colon, and so the vitamin may be released and become bioaccessible again. This might be a good strategy for controlling the release of vitamin D in the human body, but further *in vivo* studies are needed to test this.

3.5. Interaction Between Micelle and Chitosan

Finally, we carried out an additional experiment to examine the potential interactions between chitosan and mixed micelles. In this case, chitosan was directly mixed with the mixed micelle phase formed by digestion of a pure emulsion sample. In the absence of chitosan, the mean particle diameter of the mixed micelle solution was 218 nm (Fig 8a), which is higher than that reported for simple micelles (< 10 nm). This was probably because a variety of other colloidal structures were formed during digestion under fed state conditions, including vesicles, calcium soaps, and protein aggregates [56, 57]. The addition of 0% chitosan solution (just acetic acid solution), significantly ($p < 0.05$) increased the mean particle size of the mixed micelles to 380 nm. It is possible that the acetic acid changed the ionic equilibration of the free fatty acids thereby altering the mixed micelle structure. The addition of 0.1 to 0.5% chitosan solutions reduced the mean particle size, which was similar to that of the pure micelle samples. Interestingly, the chitosan level did not appear to alter the particle size.

We hypothesize that the cationic chitosan bound to some of the anionic mixed micelles and caused them to precipitate. As a result, only the properties of the mixed micelles remaining in the aqueous phase would be measured by the dynamic light scattering instrument. This hypothesis

was supported by measurements of the percentage of sediment formed, with the amount increasing from 0.09% at 0% chitosan to 0.4% at 0.5% chitosan (Fig. 8b). This hypothesis is also supported by the surface potential measurements, which showed that the colloidal particles in the mixed micelle phase were strongly negatively charged at all chitosan levels (Fig 8c). Any mixed micelles that bind to the chitosan are neutralized and precipitate, and are therefore not measured by the ζ-potential instrument.

The sedimentation of the mixed micelles in the presence of chitosan also influenced the location of the vitamin D in the system (Fig. 8d). The addition of chitosan significantly ($p < 0.05$) reduced the amount of vitamin D in the supernatant phase from 93.3% at 0% chitosan to 65.9% at 0.1% chitosan (Fig 8d). Further addition of chitosan led to a further slight decrease in the percentage of vitamin D in the supernatant phase, reaching 63.3%. These results therefore support the bioaccessibility data discussed above. They suggest that chitosan binds to the vitamin-D loaded mixed micelles causing them to sediment, thereby reducing their bioaccessibility.

4. Conclusions

In this study, the impact of chitosan addition (0-0.5%) on the gastrointestinal fate of vitamin-loaded oil-in-water emulsions was examined. In particular, the effects of chitosan on the extent of lipid digestion and the bioaccessibility of vitamin D_3 were investigated. The recently updated standardized INFOGEST protocol was used to simulate the conditions in the upper regions of the human gastrointestinal tract. Chitosan induced severe droplet flocculation in the small intestine phase but this did not reduce the total amount of free fatty acids released by the end of digestion. Indeed, the oil droplets in all the emulsions were fully digested, regardless of the amount of chitosan present. It is important to note that a fraction of the free fatty acids

473 released were not completely ionized under neutral pH conditions, and so a back titration was
474 required to measure the total amount of free fatty acids released. Comparison of the results with
475 and without the back-titration suggested that chitosan altered the ionization state of the free fatty
476 acids. The presence of chitosan (0.1 to 0.5%) decreased the bioaccessibility of vitamin D_3 by
477 about 40% when compared to the samples containing no chitosan, with the chitosan level used
478 not having a major effect. As the triglycerides in all the samples were fully digested, we
479 attribute the reduction in vitamin bioaccessibility to the ability of chitosan to modulate the
480 micellization process. Cationic chitosan molecules bind to anionic vitamin-loaded mixed
481 micelles, leading to the formation of insoluble precipitates that are removed from the mixed
482 micelle phase. Our results therefore suggest that incorporating chitosan into foods as a functional
483 ingredient could have a negative impact on vitamin bioaccessibility. However, *in vivo*
484 experiments are required to determine whether the same effect occurs under more realistic
485 gastrointestinal conditions.
486

487 ## Acknowledgements

488 This material was partly based upon work supported by the National Institute of Food and
489 Agriculture, USDA, Massachusetts Agricultural Experiment Station (MAS00491). We also
490 thank the Chinese Scholarship Council (2017- 06150098) for support.
491

References

1.D. J. McClements, *Future Foods: How Modern Science is Transforming the Way We Eat*, Springer Scientic, Njew York, NY, 2019.

2.M. N. Corstens, C. C. Berton-Carabin, R. de Vries, F. J. Troost, A. A. M. Masclee and K. Schroen, Food-grade micro-encapsulation systems that may induce satiety via delayed lipolysis: A review, *Critical Reviews in Food Science and Nutrition*, 2017, **57**, 2218-2244.

3.P. J. Lillford, The impact of food structure on taste and digestibility, *Food & Function*, 2016, **7**, 4131-4136.

4.D. J. McClements, Enhanced delivery of lipophilic bioactives using emulsions: a review of major factors affecting vitamin, nutraceutical, and lipid bioaccessibility, *Food & Function*, 2018, **9**, 22-41.

5.M. Yokoyama, H. Origasa, M. Matsuzaki, Y. Matsuzawa, Y. Saito, Y. Ishikawa, S. Oikawa, J. Sasaki, H. Hishida, H. Itakura, T. Kita, A. Kitabatake, N. Nakaya, T. Sakata, K. Shimada and K. Shirato, Effects of eicosapentaenoic acid on major coronary events in hypercholesterolaemic patients (JELIS): a randomised open-label, blinded endpoint analysis, *The Lancet*, 2007, **369**, 1090-1098.

6.J. W. Pike and S. Christakos, Biology and mechanisms of action of the vitamin D hormone, *Endocrinology and Metabolism Clinics of North America*, 2017, **46**, 815-843.

7.A. N. Moulas and M. Vaiou, Vitamin D fortification of foods and prospective health outcomes, *Journal of Biotechnology*, 2018, **285**, 91-101.

8.F. Alshahrani and N. Aljohani, Vitamin D: deficiency, sufficiency and toxicity, *Nutrients*, 2013, **5**, 3605-3616.

9.H. A. Morris, Vitamin D: can you have too much of a good thing in chronic kidney disease?, *Kidney International*, 2015, **88**, 936-938.

10. S. Pilz, W. Marz, K. D. Cashman, M. E. Kiely, S. J. Whiting, M. F. Holick, W. B. Grant, P. Pludowski, M. Hiligsmann, C. Trummer, V. Schwetz, E. Lerchbaum, M. Pandis, A. Tomaschitz, M. R. Grubler, M. Gaksch, N. Verheyen, B. W. Hollis, L. Rejnmark, S. N. Karras, A. Hahn, H. A. Bischoff-Ferrari, J. Reichrath, R. Jorde, I. Elmadfa, R. Vieth, R. Scragg, M. S. Calvo, N. M. van Schoor, R. Bouillon, P. Lips, S. T. Itkonen, A. R. Martineau, C. Lamberg-Allardt and A. Zittermann, Rationale and Plan for Vitamin D Food Fortification: A Review and Guidance Paper, *Front Endocrinol (Lausanne)*, 2018, **9**, 373.

11. N. Veronese, M. Solmi, M. G. Caruso, G. Giannelli, A. R. Osella, E. Evangelou, S. Maggi, L. Fontana, B. Stubbs and I. Tzoulaki, Dietary fiber and health outcomes: an umbrella review of systematic reviews and meta-analyses, *The American Journal of Clinical Ntrition*, 2018, **107**, 436-444.

12. A. Lovegrove, C. H. Edwards, I. De Noni, H. Patel, S. N. El, T. Grassby, C. Zielke, M. Ulmius, L. Nilsson, P. J. Butterworth, P. R. Ellis and P. R.

Shewry, Role of polysaccharides in food, digestion, and health, *Critical Reviews in Food Science and Nutrition*, 2017, **57**, 237-253.

13. A. Reynolds, J. Mann, J. Cummings, N. Winter, E. Mete and L. Te Morenga, Carbohydrate quality and human health: a series of systematic reviews and meta-analyses, *Lancet*, 2019, **393**, 434-445.

14. M. J. Gidley and G. E. Yakubov, Functional categorisation of dietary fibre in foods: Beyond 'soluble' vs 'insoluble', *Trends in Food Science & Technology*, 2019, **86**, 563-568.

15. J. Singh, R. Metrani, S. R. Shivanagoudra, G. K. Jayaprakasha and B. S. Patil, Review on Bile Acids: Effects of the Gut Microbiome, Interactions with Dietary Fiber, and Alterations in the Bioaccessibility of Bioactive Compounds, *Journal of Agricultural and Food Chemistry*, 2019, **67**, 9124-9138.

16. M. M. Wang, S. Wichienchot, X. W. He, X. Fu, Q. Huang and B. Zhang, In vitro colonic fermentation of dietary fibers: Fermentation rate, short-chain fatty acid production and changes in microbiota, *Trends in Food Science & Technology*, 2019, **88**, 1-9.

17. X. Qi, F. H. Al-Ghazzewi and R. F. Tester, Dietary Fiber, Gastric Emptying, and Carbohydrate Digestion: A Mini-Review, *Starch - Stärke*, 2018, **70**, 1700346.

18. D. So, K. Whelan, M. Rossi, M. Morrison, G. Holtmann, J. T. Kelly, E. R. Shanahan, H. M. Staudacher and K. L. Campbell, Dietary fiber intervention on gut microbiota composition in healthy adults: a systematic review and meta-analysis, *The American Journal of Clinical Nutrition*, 2018, **107**, 965-983.

19. K. Makki, E. C. Deehan, J. Walter and F. Backhed, The Impact of Dietary Fiber on Gut Microbiota in Host Health and Disease, *Cell Host & Microbe*, 2018, **23**, 705-715.

20. B. Zeeb, C. L. Lopez-Pena, J. Weiss and D. J. McClements, Controlling lipid digestion using enzyme-induced crosslinking of biopolymer interfacial layers in multilayer emulsions, *Food Hydrocolloids*, 2015, **46**, 125-133.

21. D. Qin, X. Yang, S. Gao, J. Yao and D. J. McClements, Influence of dietary fibers on lipid digestion: Comparison of single-stage and multiple-stage gastrointestinal models, *Food Hydrocolloids*, 2017, **69**, 382-392.

22. Y. Li, M. Hu, Y. Du and D. J. McClements, Controlling lipid nanoemulsion digestion using nanolaminated biopolymer coatings, *Journal of Microencapsulation*, 2011, **28**, 166-175.

23. M. Espert, A. Salvador and T. Sanz, In vitro digestibility of highly concentrated methylcellulose O/W emulsions: rheological and structural changes, *Food & Function*, 2016, **7**, 3933-3942.

24. H. D. Silva, E. Beldíková, J. Poejo, L. Abrunhosa, A. T. Serra, C. M. M. Duarte, T. Brányik, M. A. Cerqueira, A. C. Pinheiro and A. A. Vicente,

Evaluating the effect of chitosan layer on bioaccessibility and cellular uptake of curcumin nanoemulsions, *Journal of Food Engineering*, 2019, **243**, 89-100.

25. Y. Li and D. J. McClements, Controlling lipid digestion by encapsulation of protein-stabilized lipid droplets within alginate–chitosan complex coacervates, *Food Hydrocolloids*, 2011, **25**, 1025-1033.

26. Y. Li and D. J. McClements, Modulating lipid droplet intestinal lipolysis by electrostatic complexation with anionic polysaccharides: Influence of cosurfactants, *Food Hydrocolloids*, 2014, **35**, 367-374.

27. A. Mackie, B. Bajka and N. Rigby, Roles for dietary fibre in the upper GI tract: The importance of viscosity, *Food Res. Int.*, 2016, **88**, 234-238.

28. A. M. R. Pilosof, Potential impact of interfacial composition of proteins and polysaccharides stabilized emulsions on the modulation of lipolysis. The role of bile salts, *Food Hydrocolloids*, 2017, **68**, 178-185.

29. M. D. Wilcox, I. A. Brownlee, J. C. Richardson, P. W. Dettmar and J. P. Pearson, The modulation of pancreatic lipase activity by alginates, *Food Chemistry*, 2014, **146**, 479-484.

30. E. Capuano, The behavior of dietary fiber in the gastrointestinal tract determines its physiological effect, *Critical Reviews in Food Science and Nutrition*, 2017, **57**, 3543-3564.

31. D. Qin, X. Yang, S. Gao, J. Yao and D. J. McClements, Influence of Hydrocolloids (Dietary Fibers) on Lipid Digestion of Protein-Stabilized Emulsions: Comparison of Neutral, Anionic, and Cationic Polysaccharides, *Journal of Food Science*, 2016, **81**, C1636-1645.

32. K. Kurita, Chitin and chitosan: Functional biopolymers from marine crustaceans, *Marine Biotechnology*, 2006, **8**, 203-226.

33. M. Rinaudo, Chitin and chitosan: Properties and applications, *Progress in Polymer Science*, 2006, **31**, 603-632.

34. H. K. No, S. P. Meyers, W. Prinyawiwatkul and Z. Xu, Applications of chitosan for improvement of quality and shelf life of foods: A review, *Journal of Food Science*, 2007, **72**, R87-R100.

35. B. Bellich, I. D'Agostino, S. Semeraro, A. Gamini and A. Cesaro, "The Good, the Bad and the Ugly" of Chitosans, *Marine Drugs*, 2016, **14**.

36. M. Borgogna, B. Bellich and A. Cesaro, Marine polysaccharides in microencapsulation and application to aquaculture: "from sea to sea", *Mar Drugs*, 2011, **9**, 2572-2604.

37. M. Kumar, R. A. A. Muzzarelli, C. Muzzarelli, H. Sashiwa and A. J. Domb, Chitosan chemistry and pharmaceutical perspectives, *Chem. Rev.*, 2004, **104**, 6017-6084.

38. R. Zhang, W. Wu, Z. Zhang, S. Lv, B. Xing and D. J. McClements, Impact of Food Emulsions on the Bioaccessibility of Hydrophobic Pesticide Residues in Co-Ingested Natural Products: Influence of Emulsifier and Dietary Fiber Type, *Journal of Agricultural and Food Chemistry*, 2019, **67**, 6032-6040.

614 39. M. Espinal-Ruiz, F. Parada-Alfonso, L. P. Restrepo-Sanchez, C. E.
615 Narvaez-Cuenca and D. J. McClements, Impact of dietary fibers [methyl cellulose,
616 chitosan, and pectin] on digestion of lipids under simulated gastrointestinal
617 conditions, *Food & Function*, 2014, **5**, 3083-3095.
618 40. S. Mun, E. A. Decker, Y. Park, J. Weiss and D. J. McClements,
619 Influence of interfacial composition on in vitro digestibility of emulsified lipids:
620 Potential mechanism for chitosan's ability to inhibit fat digestion, *Food Biophys.*,
621 2006, **1**, 21-29.
622 41. A. Brodkorb, L. Egger, M. Alminger, P. Alvito, R. Assuncao, S.
623 Ballance, T. Bohn, C. Bourlieu-Lacanal, R. Boutrou, F. Carriere, A. Clemente, M.
624 Corredig, D. Dupont, C. Dufour, C. Edwards, M. Golding, S. Karakaya, B. Kirkhus,
625 S. Le Feunteun, U. Lesmes, A. Macierzanka, A. R. Mackie, C. Martins, S. Marze,
626 D. J. McClements, O. Menard, M. Minekus, R. Portmann, C. N. Santos, I. Souchon,
627 R. P. Singh, G. E. Vegarud, M. S. J. Wickham, W. Weitschies and I. Recio,
628 INFOGEST static in vitro simulation of gastrointestinal food digestion, *Nature*
629 *Protocols*, 2019, **14**, 991-1014.
630 42. R. Zhang, W. Wu, Z. Zhang, Y. Park, L. He, B. Xing and D. J.
631 McClements, Effect of the composition and structure of excipient emulsion on the
632 bioaccessibility of pesticide residue in agricultural products, *Journal of Agricultural*
633 *and Food Chemistry*, 2017, **65**, 9128-9138.
634 43. A. H. Saberi and D. J. McClements, Fabrication of protein
635 nanoparticles and microparticles within water domains formed in surfactant–oil–
636 water mixtures: Phase inversion temperature method, *Food Hydrocolloids*, 2015,
637 **51**, 441-448.
638 44. Y. Tan, J. Liu, H. Zhou, J. Muriel Mundo and D. J. McClements,
639 Impact of an indigestible oil phase (mineral oil) on the bioaccessibility of vitamin
640 D3 encapsulated in whey protein-stabilized nanoemulsions, *Food Res. Int.*, 2019,
641 **120**, 264-274.
642 45. D. Guzey and D. J. McClements, Formation, stability and properties
643 of multilayer emulsions for application in the food industry, *Advances in Colloid*
644 *and Interface Science*, 2006, **128-130**, 227-248.
645 46. S. Mun, E. A. Decker and D. J. McClements, Influence of droplet
646 characteristics on the formation of oil-in-water emulsions stabilized by surfactant-
647 chitosan layers, *Langmuir*, 2005, **21**, 6228-6234.
648 47. S. Ogawa, E. A. Decker and D. J. McClements, Production and
649 characterization of O/W emulsions containing cationic droplets stabilized by
650 lecithin-chitosan membranes, *Journal of Agricultural and Food Chemistry*, 2003,
651 **51**, 2806-2812.
652 48. H. N. Xu, Y. Liu and L. Zhang, Salting-out and salting-in: competitive
653 effects of salt on the aggregation behavior of soy protein particles and their
654 emulsifying properties, *Soft Matter*, 2015, **11**, 5926-5932.

49. J. Combrinck, A. Otto and J. du Plessis, Whey protein/polysaccharide-stabilized emulsions: Effect of polymer type and pH on release and topical delivery of salicylic acid, *AAPS PharmSciTech*, 2014, **15**, 588-600.

50. C. Qian, E. A. Decker, H. Xiao and D. J. McClements, Nanoemulsion delivery systems: influence of carrier oil on beta-carotene bioaccessibility, *Food Chemistry*, 2012, **135**, 1440-1447.

51. P. Sassene, K. Kleberg, H. D. Williams, J. C. Bakala-N'Goma, F. Carriere, M. Calderone, V. Jannin, A. Igonin, A. Partheil, D. Marchaud, E. Jule, J. Vertommen, M. Maio, R. Blundell, H. Benameur, C. J. H. Porter, C. W. Pouton and A. Mullertz, Toward the Establishment of Standardized In Vitro Tests for Lipid-Based Formulations, Part 6: Effects of Varying Pancreatin and Calcium Levels, *The AAPS Journal*, 2014, **16**, 1344-1357.

52. C. Zhang, W. Xu, W. Jin, B. R. Shah, Y. Li and B. Li, Influence of anionic alginate and cationic chitosan on physicochemical stability and carotenoids bioaccessibility of soy protein isolate-stabilized emulsions, *Food Res. Int.*, 2015, **77**, 419-425.

53. L. G. Gómez-Mascaraque, C. Soler and A. Lopez-Rubio, Stability and bioaccessibility of EGCG within edible micro-hydrogels. Chitosan vs. gelatin, a comparative study, *Food Hydrocolloids*, 2016, **61**, 128-138.

54. S. Lv, J. Gu, R. Zhang, Y. Zhang, H. Tan and D. J. McClements, Vitamin E encapsulation in plant-based nanoemulsions fabricated using dual-channel microfluidization: Formation, stability, and bioaccessibility, *Journal of Agricultural and Food Chemistry*, 2018, **66**, 10532-10542.

55. Q. Lin, R. Liang, A. Ye, H. Singh and F. Zhong, Effects of calcium on lipid digestion in nanoemulsions stabilized by modified starch: Implications for bioaccessibility of β -carotene, *Food Hydrocolloids*, 2017, **73**, 184-193.

56. D. G. Fatouros, I. Walrand, B. Bergenstahl and A. Mullertz, Colloidal structures in media simulating intestinal fed state conditions with and without lipolysis products, *Pharm Res*, 2009, **26**, 361-374.

57. T. Nawroth, P. Buch, K. Buch, P. Langguth and R. Schweins, Liposome formation from bile salt-lipid micelles in the digestion and drug delivery model FaSSIF(mod) estimated by combined time-resolved neutron and dynamic light scattering, *Molecular Pharmaceutics*, 2011, **8**, 2162-2172.

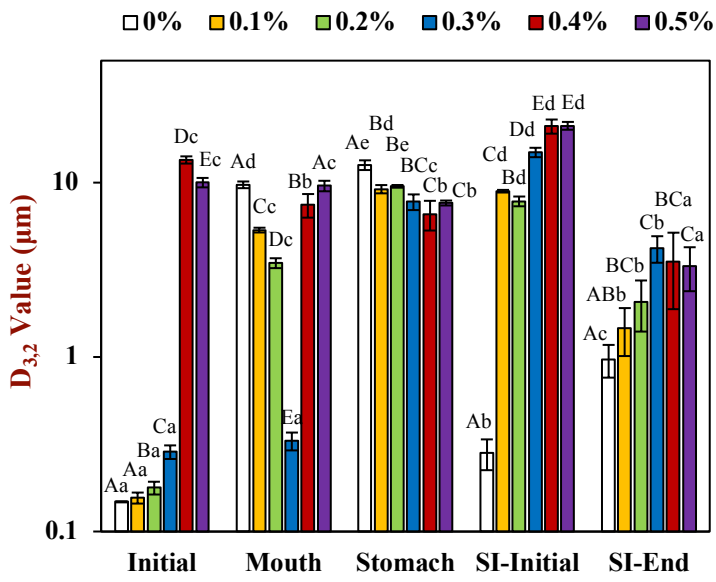

691

692 **Fig 1.** The effect of different chitosan concentrations on the surface-weighted mean particle

693 diameter ($D_{3,2}$) of the corn oil in water emulsion during stimulated gastrointestinal tract.

694 Significant difference was labeled by different capital letters (A, B, C) for different chitosan

695 concentrations (same phase), whereas lower-case letters (a, b, c) for different phases (same

696 chitosan concentration). Abbreviation: small intestine (SI).

697

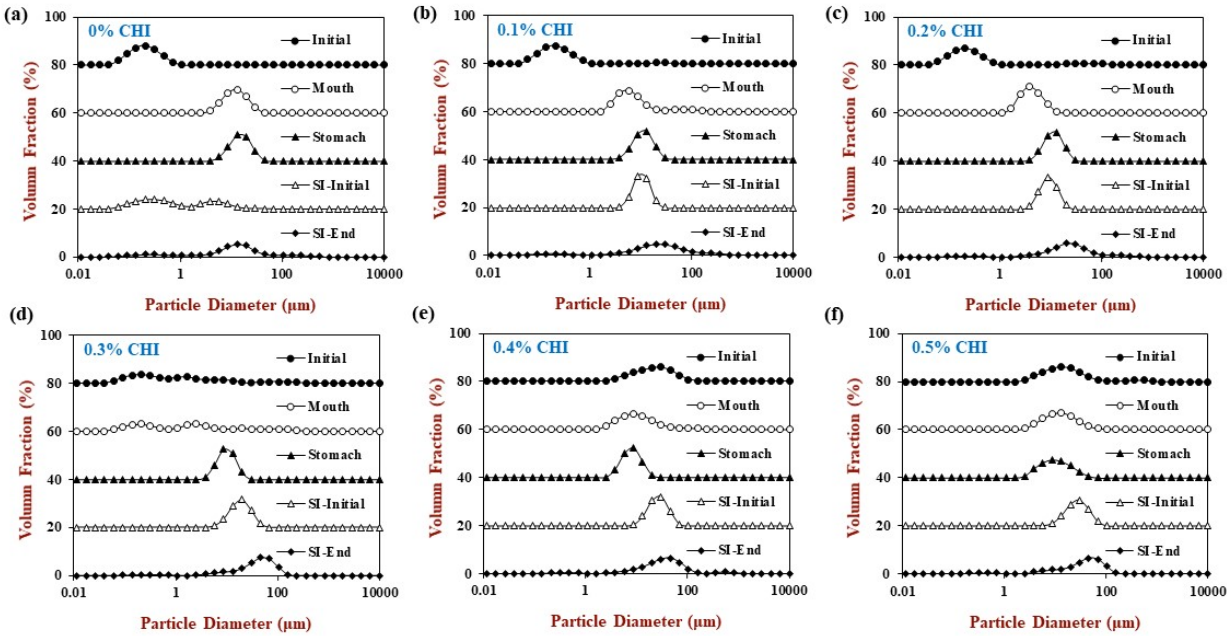

698

699 **Fig 2.** The effect of different chitosan concentrations on the particle size distribution of the corn

700 oil in water emulsion during stimulated gastrointestinal tract. Abbreviation: small intestine (SI).

701 Note: the volume fraction was stacked up the y-axis for comparison.

702

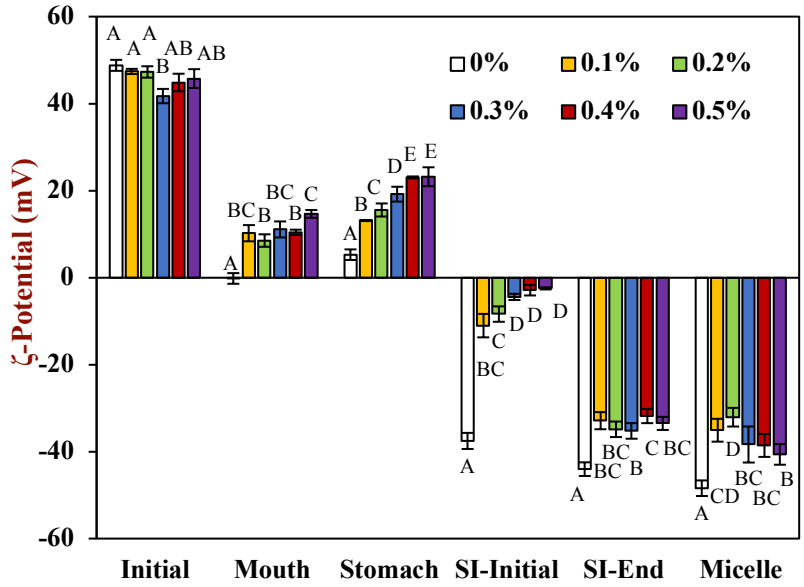

703

704 Fig 3. The effect of different chitosan concentrations on the ζ-potential of the corn oil in water

705 emulsion during stimulated gastrointestinal tract. Capital letters (A, B, C) were used for

706 distinguish significant difference of samples with different chitosan concentration (same phase).

707 Abbreviation: small intestine (SI).

708

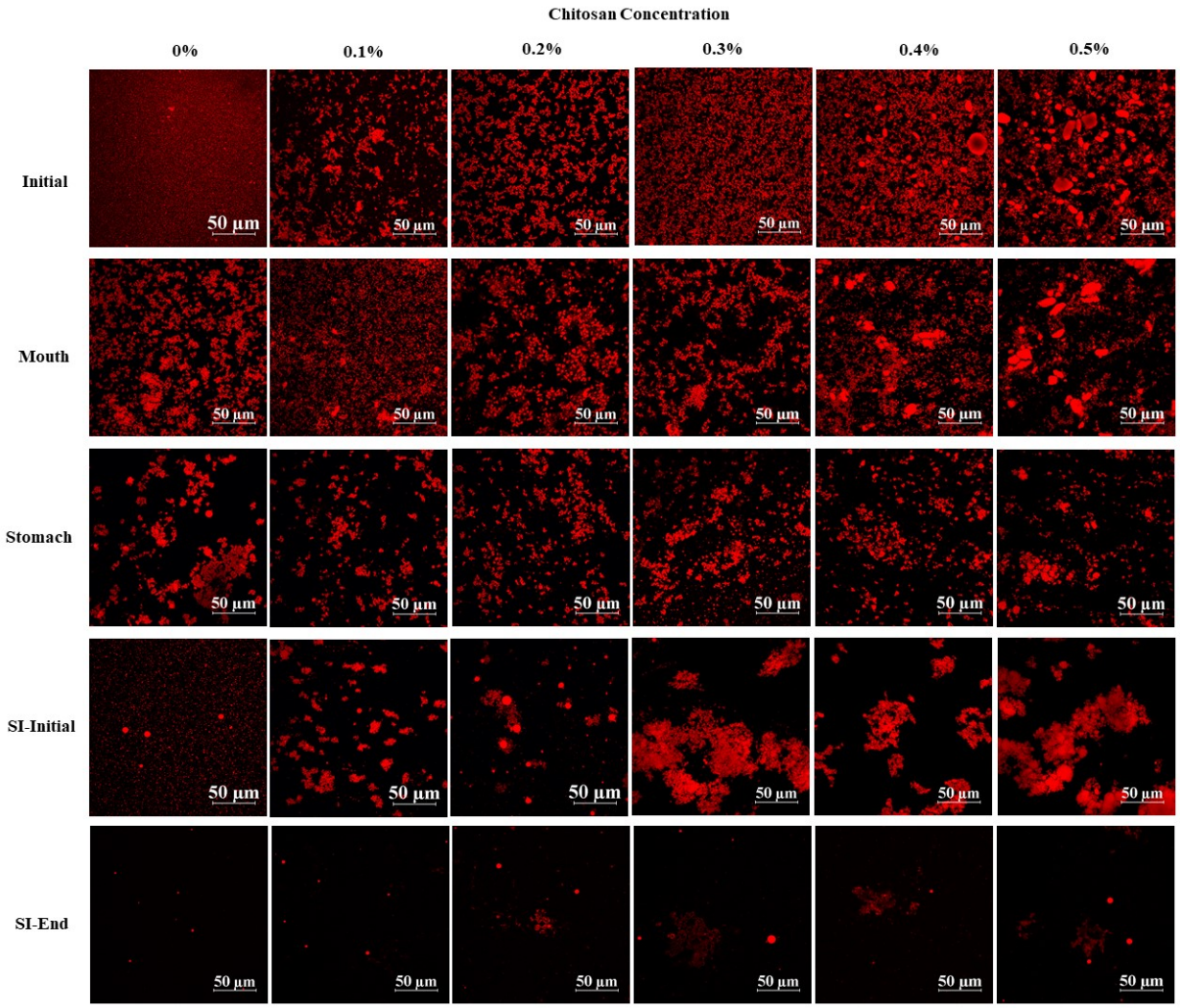

709

710 **Fig 4.** The effect of different chitosan concentrations on the confocal microscopy of the corn oil

711 in water emulsion during stimulated gastrointestinal tract. Abbreviation: small intestine (SI).

712

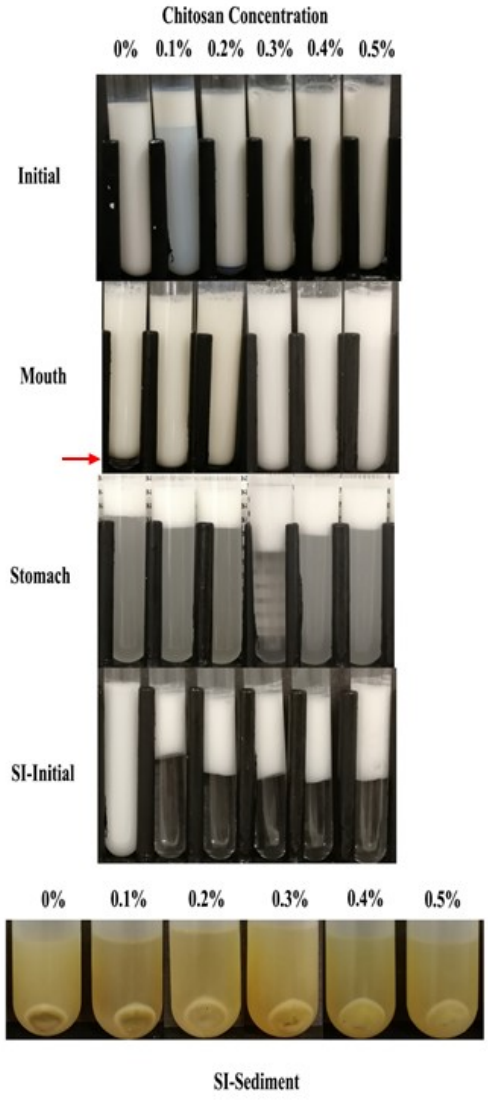

713

714 **Fig 5.** Appearance of emulsions containing different chitosan concentrations at different

715 digestive stages. *Abbreviation*: SI-initial = the initial stages of the small intestine phase.

716

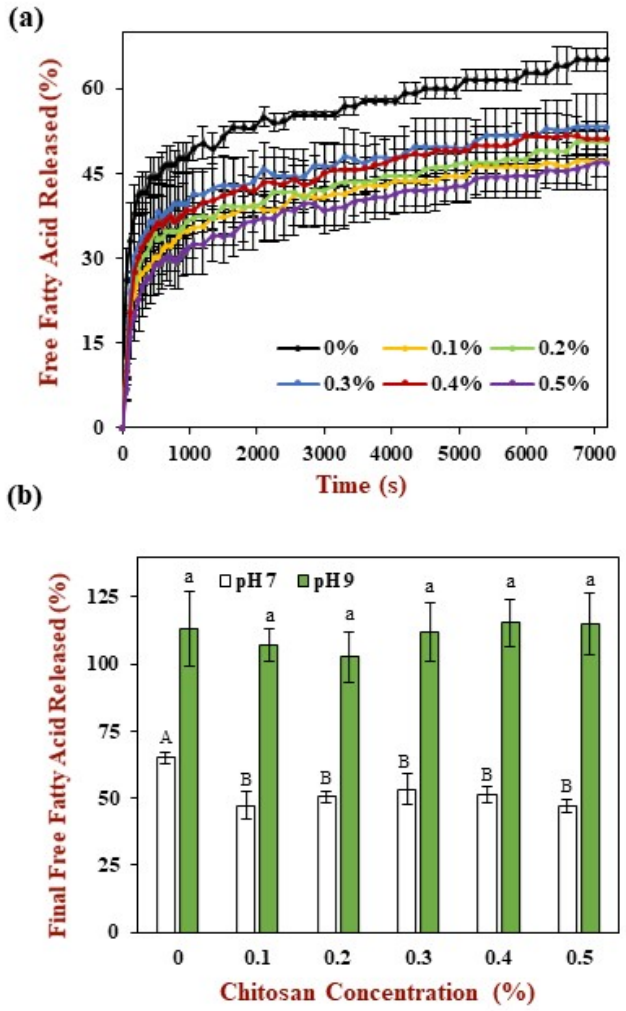

717

718 **Fig 6.** Impact of chitosan concentration on the release of free fatty acids (FFA) from corn oil-in-
719 water emulsions during simulated digestion. (a) FFA profile at pH 7, (b) final FFA value at pH 7
720 and pH 9. Capital (A, B, C) and lower-case (a, b, c) letters were used to designate significant
721 difference among different chitosan concentrations for final FFA value at pH 7 and pH 9
722 respectively.

723

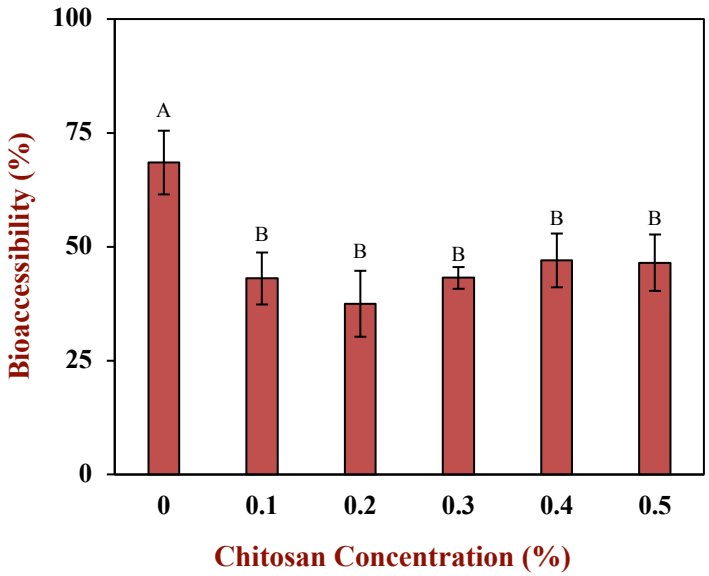

724

725 Fig 7. The effect of different chitosan concentrations on the vitamin D bioaccessibility of the
726 corn oil in water emulsion during stimulated gastrointestinal tract. Samples with significant
727 difference were labeled with different capital letters (A, B, C).

728

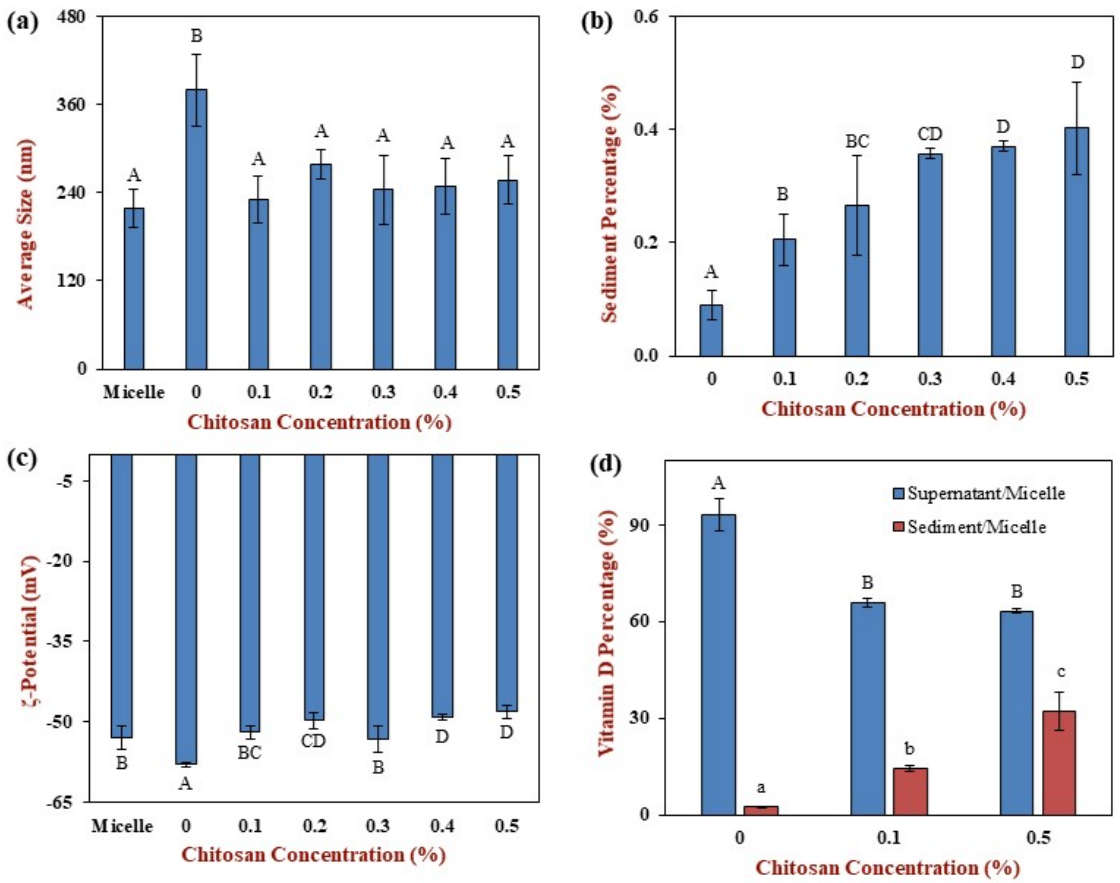

729

730 Fig 8. The effect of different chitosan concentrations on the physical properties and vitamin D
731 distribution of mixed micelles prepared from corn oil-in-water emulsions after exposure to the
732 simulated gastrointestinal tract: (a) mean particle diameter; (b) percentage of sediment formed;
733 (c) ζ-potential; (d) vitamin D percentage in supernatant or sediment. Samples with significant
734 differences were labeled with different capital letters (A, B, C), whereas samples with different
735 lower-case letters (a, b, c) were used for vitamin D percentage of sediment.

736

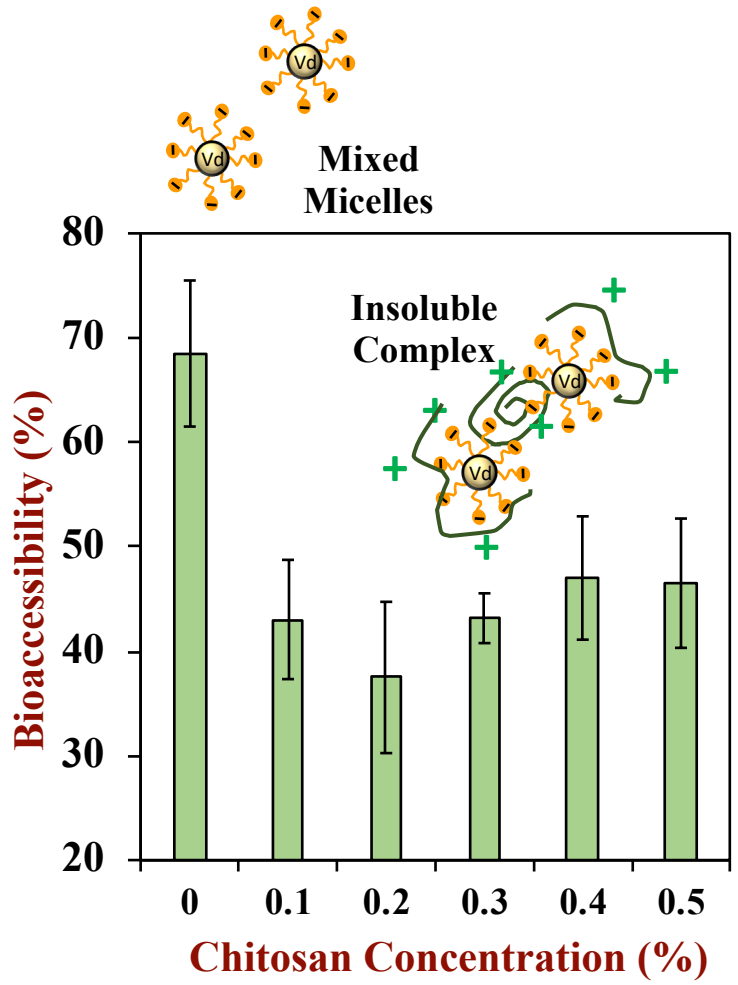
Vd
Vd
Mixed
Micelles
Insoluble
Complex
Vd
Vd
80
70
60
50
40
30
20
Bioaccessibility (%)
0
0.1
0.2
0.3
0.4
0.5
Chitosan Concentration (%)